Journal of Thermal Analysis and Calorimetry, Vol. 75 (2004) 649–654

PREPARATION AND CHARACTERIZATION OF $Co_{80}Nb_{20-x}B_x$ AMORPHOUS METALLIC RIBBONS

R. S. Castro[1*], *Shiva Prasad*[4], *R. M. Gomes*[2], *I. C. E. S. G. Lima*[2], *A. G. Souza*[3], *T. A. A. Melo*[2] *and S. J. G. Lima*[2]

[1]Centro de Educação Tecnológica Federal de Pernambuco, Recife, PE, Brazil
[2]Departamento de Tecnologia Mecânica, Universidade Federal da Paraíba, Campus I, Cidade Universitária, 58059-900 João Pessoa, Paraíba, Brazil
[3]Laboratório de Termoquímica e Materiais, CCEN-DQ, Universidade Federal da Paraíba, Campus I, Cidade Universitária, 58059-900 João Pessoa, Paraíba, Brazil
[4]Departamento de Engenharia Química, CCT, Universidade Federal de Campina Grande, Campus I, 58109-970 Campina Grande, Paraíba, Brazil

Abstract

$Co_{80}Nb_{14}B_6$, $Co_{80}Nb_{12}B_8$ and $Co_{80}Nb_{10}B_{10}$ amorphous alloys were obtained through the melt-spinning process. The ribbons structure was investigated by X-ray diffractometry and the crystallization process and the thermal stability were studied by means of differential thermal analysis and thermomechanical technique. It was observed that the crystallization temperature depends on the alloy composition and occurs in a temperature range between 420 and 730°C. The coercive field of all alloys was determined by magnetic susceptibility measurements, the values of which range from 2.78 to 5.95 A m^{-1}.

Keywords: CoNbB amorphous alloys, melt spinning and crystallization temperature

Introduction

Amorphous metallic alloys have been extensively studied since the 60's [1] due to their promising application in various industrial areas. Singular properties arise from the fact that these materials possess neither magneto-crystalline anisotropy nor grain boundaries. The properties of these alloys can be modified by their chemical composition and thermomechanical processing [2]. Among various amorphous alloys the CoNbB systems are very attractive in Brazil because of the large niobium reserves located in the states of Minas Gerais and Goiás states [3]. The CoNbB system is easy to produce and possesses low coercivity and high magnetization combined with good thermal stability [4–6]. However, the use of these alloys is limited because at high temperature these alloys crystallize from the amorphous state resulting in reduced magnetic properties. Therefore, the study of thermal stability of these materials is of major importance.

* Author for correspondence: E-mail: jackson@lsr.ct.ufpb.br

1388–6150/2004/ $ 20.00
© 2004 Akadémiai Kiadó, Budapest
Akadémiai Kiadó, Budapest
Kluwer Academic Publishers, Dordrecht

In this work, the effect of the B addition on the CoNb amorphous metallic ribbons was studied. The structural characterization of the alloys was done based on differential thermal analysis and thermomechanical experiments. The magnetic permeability and coercivity were also measured.

Experimental procedures

$Co_{80}Nb_{14}B_6$, $Co_{80}Nb_{12}B_8$ and $Co_{80}Nb_{10}B_{10}$ alloys were prepared and homogenized by high frequency induction furnace several times over a water-cooled copper chill under an argon atmosphere. High purity Co (99.9%), Nb (99.8) and Co_2B boride were used. The alloys were melt spun onto a rotating (about 1500 min^{-1}) polished copper wheel (about 3600 mm in diameter) after induction melting under argon atmosphere in a quartz nozzle with an orifice of about 0.8 mm employing an ejection pressure of about 90 KPa. The resulting ribbons were approximately 25 μm thick and 1.0 mm wide. The amorphous nature of the ribbons was investigated by X-ray diffractometry using a Siemens D5000 diffractometer with a CuK_α radiation of 0.15406 nm. The crystallization process was investigated using a Shimadzu DTA-50 differential thermal apparatus. The samples were submitted to the following heating cycle at a constant heating rate of 30 K min^{-1}: heating from room temperature up to 200°C with a soak step at 200°C for 3 min with further heating from 200 to 800°C with a soak step at 800°C for 3 min. Thermomechanical analyses were performed using a Shimadzu TMA-50 apparatus. Fifteen mm-long samples were subjected to a constant tensile load of 10 g. The ribbon samples were submitted to a heating cycle similar to the differential thermal analysis ones, except that the final temperature was changed to 950°C. The measurements of the magnetic susceptibility were done at room temperature by self-designed equipment that consists of a Princeton digital lock and power source. The ribbon samples were fixed on a quartz tube and placed in the interior of a spire, 10.0 mm in diameter and 30.0 mm long. The coercive field was calculated from the magnetic susceptibility data.

Results and discussion

The XRD patterns of the melt spun ribbons, shown in Fig. 1, clearly reveals the amorphous structures of all the $Co_{80}Nb_{20-x}B_x$ alloys.

The DTA curves of all three alloys are shown in Fig. 2. In all alloys, a reaction sequence is observed which makes it difficult to determine the onset temperature of each reaction separately. Four successive transformations can be identified for the $Co_{80}Nb_{10}B_6$ alloy, for instance. According to Betancourt [7] and Morret [8], these transformations correspond to the precipitation of nanocrystallines phase which is prevailingly constituted of pure crystal of Co and some Co compound (Co_3B, Co_2B…). However, the existence of different reactions suggests that the crystallization process of CoNbB amorphous alloys appears more complex. It can be observed that the B addition strongly influences the crystallization temperature of CoNbB amorphous alloys. The onset temperature of the first reaction, T_1, decreases with increasing the B content which indicates that

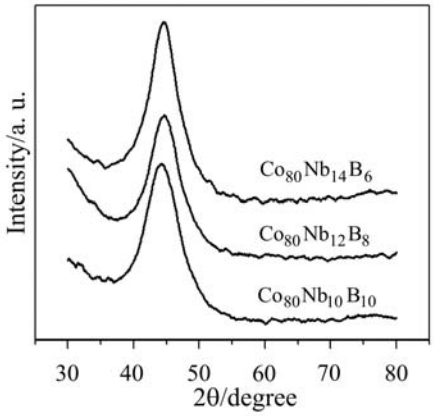

Fig. 1 XRD patterns of the melt spun ribbons

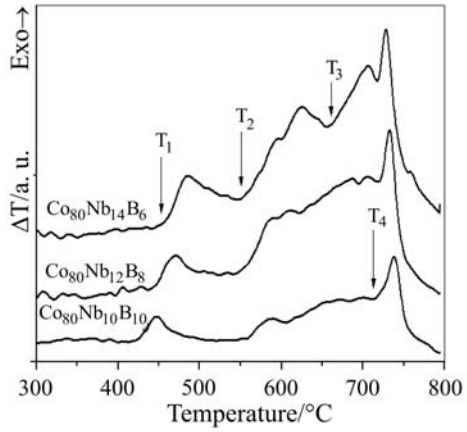

Fig. 2 Differential thermal analysis scans of the alloys

this reaction is due to the formation of some Co–B compound. Additionally, the intensity of the penultimate transformation reaction, T_3, decreases with the B content to such an extent that it is no longer observed in the $Co_{80}Nb_{10}B_{10}$ alloy. The onset temperature of the first crystallization reactions and the temperatures range of all crystallization process for each alloy were determined by the tangent line method and are listed in Table 1. It can be observed that, as the B content increases the onset and the endset temperature of crystallization decreases, suggesting that the B addition accelerates the crystallization process of the alloys. Further studies using transmission electron microscope are needed to fully clarify the precipitation sequence during crystallization process.

Figure 3 shows the thermomechanical curves of all alloys. Unlike the curves obtained DTA where a different reaction was detected, the crystallization reaction sequence is not well defined. Only two relevant changes are detected in the coefficient of thermal expansion as listed in Table 2. The first interval is between 430 to 480°C, and the second around 730°C. These values are consistent with those obtained by the

DTA technique, and probably it can be attributed to the formation of nanocrystallines phase from the amorphous structure.

Table 1 Temperatures of crystallization determined from the DTA curves (error ±3.0°C)

Sample	Onset temperature of each reaction/°C				Transformation interval
	T_1	T_2	T_3	T_4	
$Co_{80}Nb_{14}B_6$	455	556	663	720	455–743
$Co_{80}Nb_{12}B_8$	445	551	–	722	445–746
$Co_{80}Nb_{10}B_{10}$	423	559	–	713	423–754

Temperature T_1, corresponding to the inflexion point, decreases with increasing B content that is consistent with the first reaction detected in the DTA analyses. Temperature T_2 corresponds to the point where the last reaction starts. It is also observed that the coefficient of thermal expansion is much lower for the amorphous structures i.e., at temperatures lower than T_1, than for fully crystallized alloys.

Table 2 Crystallization temperatures (error ±3.0°C) obtained by TMA and coefficient of thermal expansion (CTE) before and after crystallization

Alloy	Transformation temperature/°C		CTE/10^{-6} K^{-1}	
	T_1	T_2	Temp<T_1	Temp>T_2
$Co_{80}Nb_{14}B_6$	475	735	7.5	40.2
$Co_{80}Nb_{12}B_8$	458	733	10.9	21.6
$Co_{80}Nb_{10}B_{10}$	433	739	15.0	32.8

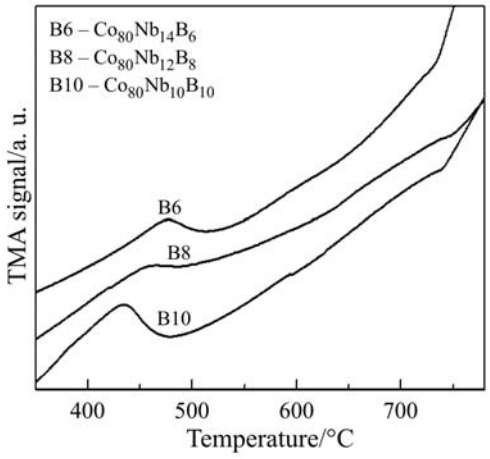

Fig. 3 TMA curves of the alloys

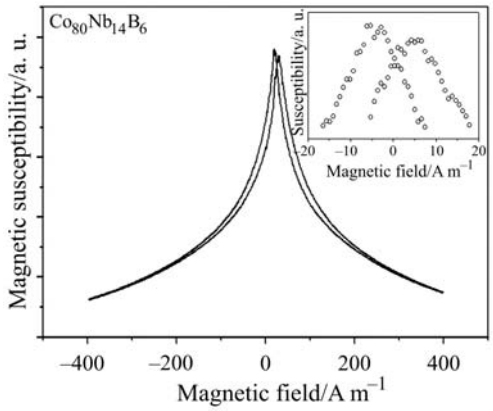

Fig. 4 Magnetic susceptibility curves obtained for the $Co_{80}Nb_{14}B_6$ alloy

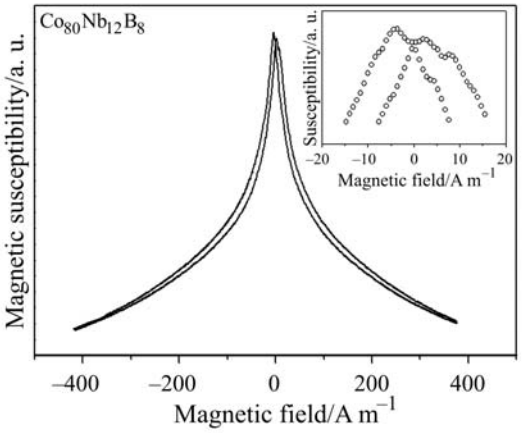

Fig. 5 Magnetic susceptibility curves obtained for the $Co_{80}Nb_{12}B_8$ alloy

In Figs 4 and 5 are the magnetic susceptibility curves obtained for the $Co_{80}Nb_{14}B_6$ and $Co_{80}Nb_{12}B_8$ alloys, as a function of the DC field applied. The coercive field (H_c), obtained by subtracting the values of H corresponding to the maximum of each curve are, respectively, 2.78 and 5.95 A m^{-1}, when the B content decreases from 8 to 6%. These values that obtained agree with those found by other researches for Co-based soft magnetic alloys [9–11].

Table 3 Magnetic permeability and coercive field of the ribbons

Alloy	μ_{max}/emu	H_c/Oe
$Co_{80}Nb_{14}B_6$	3598	0.075
$Co_{80}Nb_{12}B_8$	4143	0.035

Conclusions

$Co_{80}Nb_{14}B_6$, $Co_{80}Nb_{12}B_8$ and $Co_{80}Nb_{10}B_{10}$ alloys with amorphous structure were obtained by the melt-spinning method and their crystallization behavior was investigated by DTA and TMA. The crystallization process of the $Co_{80}Nb_{20-x}B_x$ alloys is characterized by a sequence of reactions, which occur at a temperature interval of 420 to 750°C. The substitution of niobium by boron decreases the onset temperature of crystallization and elevates the endset temperature. The crystallization reactions are more accurately determined by DTA than by TMA. The latter identifies only the onset and endset temperatures of crystallization but does not show the intermediate reactions.

The $Co_{80}Nb_{14}B_6$ and $Co_{80}Nb_{12}B_8$ alloys possess a relative maximum magnetic permeability of 3598 and 4143 emu, respectively, and display low coercivity values: 0.075 Oe for the $Co_{80}Nb_{14}B_6$ alloy and 0.035 Oe for the $Co_{80}Nb_{12}B_8$ alloy. Therefore, the increase in boron content causes an improvement in magnetic permeability and at the same time, decreases the coercivity values.

* * *

The authors are grateful to the Brazilian PADCT/CNPq and CAPES for supporting this work.

References

1 P. Duwez and F. E. Luborsky, Amorphous Metallic Alloys, New York 1983, p. 3.
2 R. Boll, H. R. Hilziger and H. Warlimont, Magnetic Material Properties and Applications of Metallic Glasses in Electronic Devices, in R. Hasegawa (Ed.), Glassy Metals; in Magnetic, Chemical and Structural Properties, (1983) 184.
3 N. P. Lyakishev, N. A. Tulin and Yu. L. Pliner, Niobium in Steels and Alloys, Ed. CBMM, São Paulo, Brazil 1984, p. 17.
4 R. C. O'Handley, B. W. Corb, Y. Hara and N. J. Grant, J. Appl. Phys., 53 (1982) 7753.
5 B. W. Corb, R. C. O'Handley, S. Paradis and N. J. Grant, J. Appl. Phys., 55 (1984) 1781.
6 T. Egami, Rep. Prog. Phys., 47 (1984) 1601.
7 I. Betancourt, M. Jiménez, S. Aburto, V. Marquina, R. Gómez, M. L. Marquina, R. Ridaura, M. Miki and R. Valenzuela, J. Magn. Magn. Mater., 140–144 (1995) 459.
8 F. Morret, Elaboration d'Alliages Microcristalisés par Dévitrification de Verres Métaliques NiNb et CoNbB Trempés sur Roleau, Grenoble, Institut National Polytechnique, PhD Thesis, (1987) 181.
9 G. Bordin, G. Buttino, A Cecchetti and M. Poppi, J. Magn. Magn. Mater., 195 (1999) 583.
10 J. H. Yang, Y. B. Kim, K. S. Ryu, M. J. Kim, Y. C. Chung and T. K. Kim, J. Magn. Magn. Mater., 222 (2000) 65.
11 A. K. Shaikh, D. Wexlers and G. W. Delamore, J. Magn. Magn. Mater., 152 (1996) 345.